Piezoelectric properties and phase transition temperatures of the solid solution of $(1-x)(Bi_{0.5}Na_{0.5})TiO_3–xSrTiO_3$

Werner Krauss [a],[*], Denis Schütz [a], Franz Andreas Mautner [b], Antonio Feteira [c], Klaus Reichmann [a]

[a] *Graz University of Technology, Christian Doppler Laboratory for Advanced Ferroic Oxides, Stremayrgasse 16, 8010 Graz, Austria*
[b] *Graz University of Technology, Institute of Physical and Theoretical Chemistry, Rechbauerstraße 12, 8010 Graz, Austria*
[c] *The University of Birmingham, School of Chemistry, Edgbaston, Birmingham B15 2TT, United Kingdom*

Abstract

The phase diagram of $(1-x)(Bi_{0.5}Na_{0.5})TiO_3–xSrTiO_3$ was completed and investigations on polarization and strain in this system were carried out. $(1-x)(Bi_{0.5}Na_{0.5})TiO_3–xSrTiO_3$-ceramics were prepared by conventional mixed oxide processing. The depolarization temperature (T_d), the temperature of the rhombohedral–tetragonal phase transition (T_{r-t}) and the Curie temperature (T_m) were determined by measuring the temperature dependence of the relative permittivity. All solid solutions of $(1-x)(Bi_{0.5}Na_{0.5})TiO_3–xSrTiO_3$ show relaxor behavior (A-site relaxor). From XRD-measurements a broad maximum of the lattice parameter can be observed around $x = 0.5$ but no structural evidence for a morphotropic phase boundary was found. SEM-analysis revealed a decrease of the grain size for increasing $SrTiO_3$-content. At room temperature a maximum of strain of about 0.29% was found at $x = 0.25$ which coincides with a transition from a ferroelectric to an antiferroelectric phase. The temperature dependence of the displacement indicates an additional contribution from a structural transition (rhombohedral–tetragonal), which would be of certain relevance for the existence of a morphotropic phase boundary.

1. Introduction

$(Bi_{0.5}Na_{0.5})TiO_3$ (BNT) is one of the most investigated lead-free piezoelectric materials.[1,2] It has a perovskite type structure with rhombohedral symmetry (R3C) at room temperature. The depolarization temperature (T_d) is at 186 °C and the Curie temperature (T_m) at 335 °C. T_d and T_m both can be shifted by doping[3] or by the formation of solid solutions with alkaline earth titanates.[3,4] $Bi_{0.5}Na_{0.5}TiO_3$ shows strong ferroelectricity ($P_r = 38\ \mu C/cm^2$), but it also has drawbacks like a large coercive field of about 7 kV/mm, which leads to problems in the poling process. To overcome these problems and to optimize the properties of $Bi_{0.5}Na_{0.5}TiO_3$ solid solutions with other lead-free materials can be used. In combination with compounds of tetragonal symmetry (e.g. $BaTiO_3$ and $(Bi_{0.5}K_{0.5})TiO_3$)[5–11] the solid solution system with $Bi_{0.5}Na_{0.5}TiO_3$ exhibits a morphotropic phase boundary (MPB). It is known that morphotropic

phase boundaries lead to higher values of d_{33} and k_{33}. For the solid solution $(1-x)(Bi_{0.5}Na_{0.5})TiO_3–xBaTiO_3$ the morphotropic phase boundary is found at $x = 0.06$ with a minimum in T_d at about 100 °C.

$SrTiO_3$ has a perovskite type structure and a cubic symmetry at room temperature. Below −168 °C a transition to tetragonal symmetry is reported by Jauch and Palmer.[12] Hypothetically there is the possibility to observe a phase transition from a rhombohedral to tetragonal phase in solid solutions with $Bi_{0.5}Na_{0.5}TiO_3$. In all known cases of a morphotropic phase boundary in solid solutions of $Bi_{0.5}Na_{0.5}TiO_3$ and a tetragonal phase the depolarization temperature as well as the Curie temperature exhibit a minimum. Out of this reason it is necessary in the system $(1-x)(Bi_{0.5}Na_{0.5})TiO_3–xSrTiO_3$ to measure at low temperatures to observe a phase transition from a rhombohedral to a tetragonal phase. A phase diagram (Fig. 1) of $(1-x)(Bi_{0.5}Na_{0.5})TiO_3–xSrTiO_3$ published by Watanabe et al.[4] exists up to $x = 0.25$. Watanabe used the maxima in the permittivity vs. temperature curves measured at a frequency of 10 kHz. The first maximum at lowest temperature, called the depolarization temperature (T_d) is connected to the

* Corresponding author. Tel.: +43 316 873 8270; fax: +43 316 873 8272.
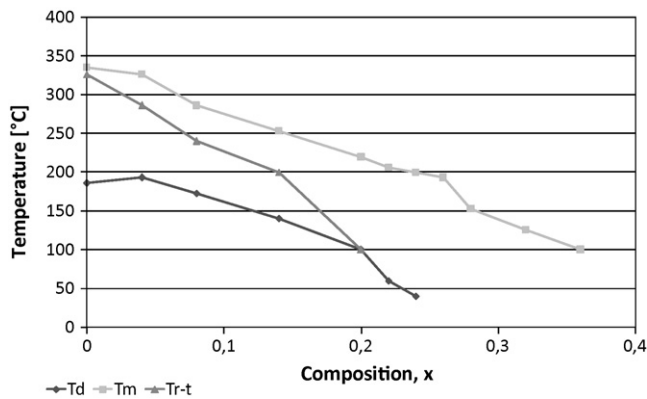*E-mail address:* werner.krauss@tugraz.at (W. Krauss).

Fig. 1. Dielectric transitions for $(1-x)(Bi_{0.5}Na_{0.5})TiO_3-xSrTiO_3$ (data published by Watanabe et al.[4]) (depolarization temperature (T_d), rhombohedral–tetragonal phase transition temperature (T_{r-t}) and the temperature (T_m) of the maximum dielectric constant for x in $(1-x)(Bi_{0.5}Na_{0.5})TiO_3-x$ $SrTiO_3$.

ferroelectric/antiferroelectric phase transition, the maximum at the highest temperature assigned to the Curie temperature (T_m) is associated with the transition from antiferroelectric to paraelectric. Between these two transition temperatures Watanabe identified a third transition temperature, which he called rhombohedral–tetragonal phase transition temperature (T_{r-t}). Just recently Hiruma et al.[13] verified a very small tetragonal distortion in pure BNT above this T_{r-t}, which supports Watanabes hypothesis.

Hiruma et al.[14] also found a strain maximum in the system $(1-x)(Bi_{0.5}Na_{0.5})TiO_3-xSrTiO_3$ at $x=0.26$ and they suggested that a morphotropic phase boundary is the reason for the large strain. Because of obvious differences to the characteristic features of the system BNT-BT we decided to complete the phase diagram over the whole composition range and look for structural and dielectric features that would support the existence of a morphotropic phase boundary.

2. Experimental procedure

The samples were prepared by a conventional mixed oxide process. In the first step a $Bi_{0.5}Na_{0.5}TiO_3$ master batch was made from bismuth oxide (reagent grade, HEK-Oxide GmbH), sodium carbonate (reagent grade, Merck) and titanium oxide (reagent grade, Bayer). After the first calcination at 850 °C the $Bi_{0.5}Na_{0.5}TiO_3$ was weighted together with strontium carbonate (reagent grade, Solvay) and titanium oxide in the chosen stoichiometry. After milling in a planetary mill (Fritsch Pulverisette 4) a second calcination took place at 850 °C. The powder was milled again and out of the dried powder a granulate was made by adding 5% polyethylene glycol 20 000 as a binder. The granulate was sieved and discs with a diameter of 13 mm were uniaxially cold pressed with a load of 2 tonnes. The discs were decarbonised at 450 °C and then sintered between 1200 and 1300 °C for 2 h. The proper sintering temperature was determined by dilatometry (*NETZSCH DIL 402 C*). Samples with a SrTiO_3-content up to $x=0.5$ were sintered at 1200 °C, for higher SrTiO_3-content 1300 °C was used.

The sintered discs were gold sputtered for contacting. The X-ray powder data were collected in the reflection mode at room temperature and −243 °C with a Philips Expert diffractometer using Cu/Kα radiation. The cooling equipment was a closed cycle He cryostat (He-TTK Anton Paar) with cooling range between −263 and +27 °C. Data sets were collected from 20° to 80° (2-theta), step-width = 0.02° (2-theta) and step-time = 20 s/step. The lattice parameters were determined by Rietveld refinement using Philips Expert software. The temperature dependence of the relative permittivity was measured in the temperature range of −50 °C to 300 °C using Novocontrol Concept 40. The samples with $x=0.8$ and 0.9 were measured from −243 °C to room temperature using an LCR bridge (Model E4980A, Agilent) coupled to a closed-circuit He-Cryocooler (Model CC 2.5 Oxford Instruments). For all samples the frequencies 1 kHz, 10 kHz and 100 kHz were used. The polarization and displacement curves were measured with aixPES (Piezoelectric Evaluation System from aixACCT) from room temperature to 150 °C.

3. Results and discussion

For identification of structural changes throughout the composition range we carried out low temperature XRD-measurements at −243 °C to identify an expected transition between rhombohedral and tetragonal phase. In our XRD-spectra of $(1-x)(Bi_{0.5}Na_{0.5})TiO_3-xSrTiO_3$ (Fig. 2) we could not detect any tetragonal distortion, even not for pure SrTiO_3. We concluded, that the tetragonal distortion in the system $(1-x)(Bi_{0.5}Na_{0.5})TiO_3-xSrTiO_3$ is too small to be detected within the resolution of the equipment available.

The calculated lattice parameters (for cubic indexing) are in good agreement with literature data. In Fig. 3 one can see that there is a broad maximum of the lattice parameter around $x=0.5$. The decrease of the lattice parameter for $x>0.5$ cannot be interpreted by Vegards law which would postulate a steady increase of the lattice parameter because the ionic radius of strontium is larger than either bismuth or sodium. The differences of the lattice parameters measured at −243 °C and at room temperature, which are in the range of the thermal expansion,
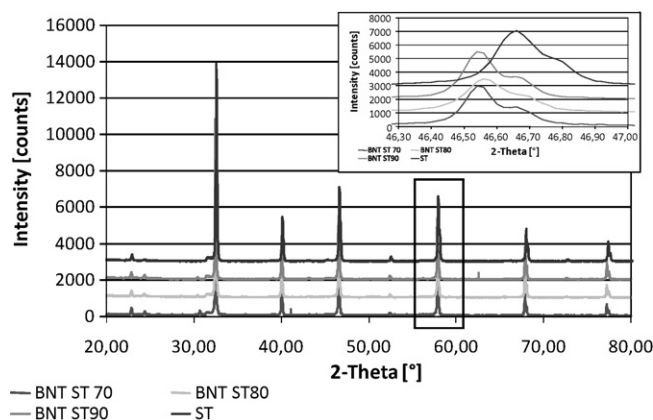

Fig. 2. XRD-spectra of $(1-x)(Bi_{0.5}Na_{0.5})TiO_3-xSrTiO_3$ for $x=0.7$ (BNT ST 70), $x=0.8$ (BNT ST 80), $x=0.9$ (BNT ST 90) and $x=1.0$ (ST) at −243 °C.

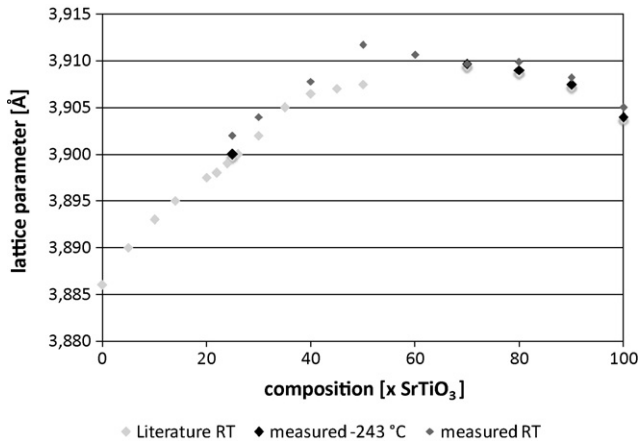Fig. 3. Lattice parameters for $(1-x)(Bi_{0.5}Na_{0.5})TiO_3$–$xSrTiO_3$ (literature data from Park and Hong[15]).
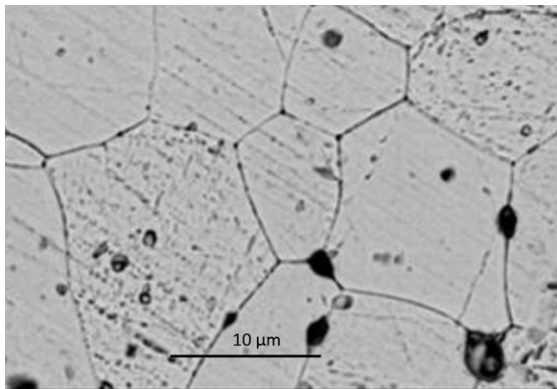

Fig. 4. Microstructure of $0.90(Bi_{0.5}Na_{0.5})TiO_3$–$0.10SrTiO_3$ (SEM-image).

do not support any significant structural changes, that would give evidence for a morphotropic phase boundary in the system $(1-x)(Bi_{0.5}Na_{0.5})TiO_3$–$xSrTiO_3$.

With the applied preparation conditions we achieved dense ceramics as one can see in micrographs of polished and etched samples (Figs. 4–7). The formation of a solid solution with $SrTiO_3$ strongly influences the microstructure of the $Bi_{0.5}Na_{0.5}TiO_3$-ceramic. The grain size of the system $(1-x)(Bi_{0.5}Na_{0.5})TiO_3$–$xSrTiO_3$ decreases from
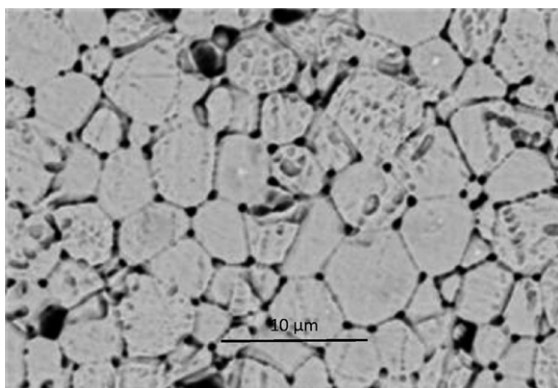

Fig. 5. Microstructure of $0.73(Bi_{0.5}Na_{0.5})TiO_3$–$0.27SrTiO_3$ (SEM-image).
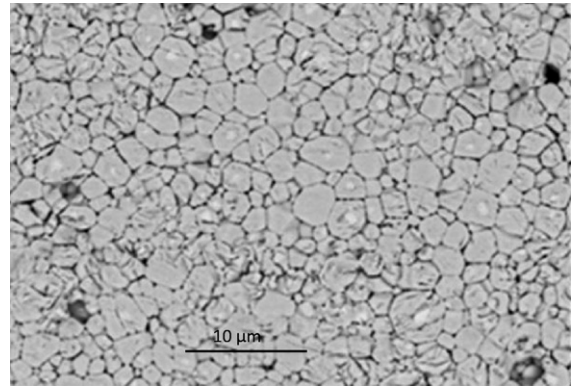

Fig. 6. Microstructure of $0.60(Bi_{0.5}Na_{0.5})TiO_3$–$0.40SrTiO_3$ (SEM-image).
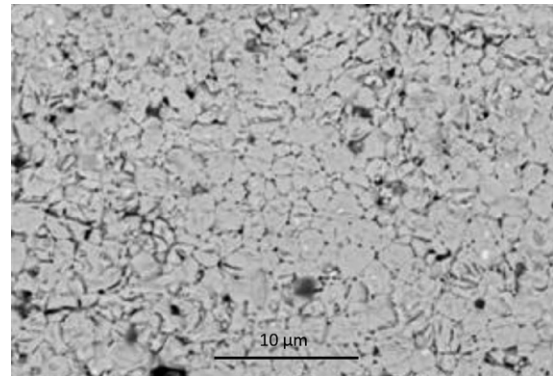
Fig. 7. Microstructure of $0.10(Bi_{0.5}Na_{0.5})TiO_3$–$0.90SrTiO_3$ (SEM-image).

approximately $10\,\mu m$ for $x = 0.1$ to a grain size of around $3\,\mu m$ for $x = 0.9$.

On the temperature dependence of the relative permittivity (Figs. 8–11) the maximum at the highest temperature was assigned to the Curie temperature T_m, the maximum at the lowest temperature to the depolarization temperature T_d. Maxima in between ($T_{r–t}$) were assigned to a rhombohedral/tetragonal phase transition according to the nomenclature used by Watanabe et al.[4] For $x > 0.23$ $T_{r–t}$ coincides with T_d, for $x > 0.60$ only one maximum is observed, which is assigned to T_m. One can see that there is a frequency dependence of the
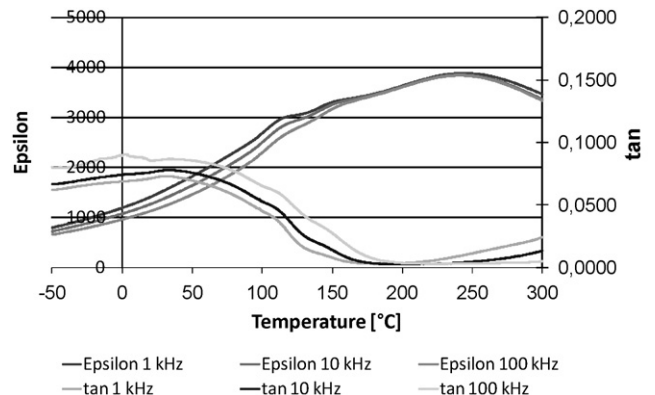

Fig. 8. Temperature dependence of the relative permittivity of $0.80(Bi_{0.5}Na_{0.5})TiO_3$–$0.20SrTiO_3$.
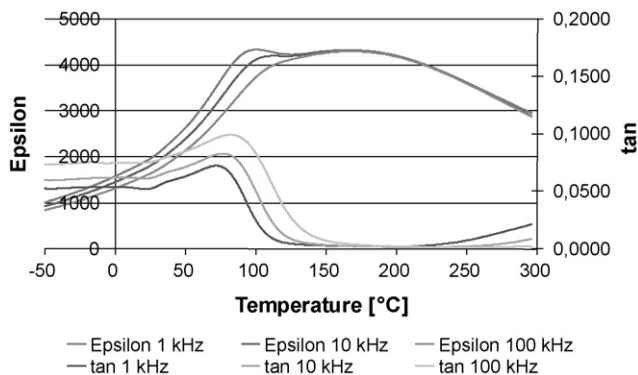
Fig. 9. Temperature dependence of the relative permittivity of $0.70(Bi_{0.5}Na_{0.5})TiO_3$–$0.30SrTiO_3$.

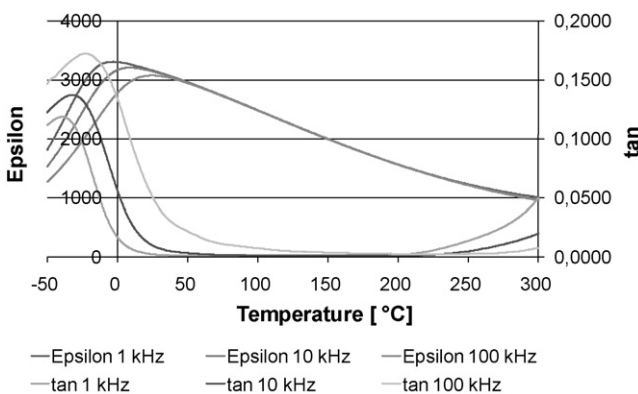Fig. 10. Temperature dependence of the relative permittivity of $0.40(Bi_{0.5}Na_{0.5})TiO_3$–$0.60SrTiO_3$.

depolarization temperature T_d up to $x = 0.6$. On samples with $x > 0.6$ we find frequency dependence of the Curie temperature (T_m). From that we can state that all solid solutions of $(1 - x)(Bi_{0.5}Na_{0.5})TiO_3$–$xSrTiO_3$ exhibit relaxor behavior (A-site relaxor).

In accordance to Watanabe we used the permittivity data at 10 kHz to plot the phase diagram (Fig. 12). The phase diagram shows, that the Curie temperature T_m decreases almost linearly with increasing $SrTiO_3$-content to $-144\,^\circ C$ at $x = 0.9$. Between
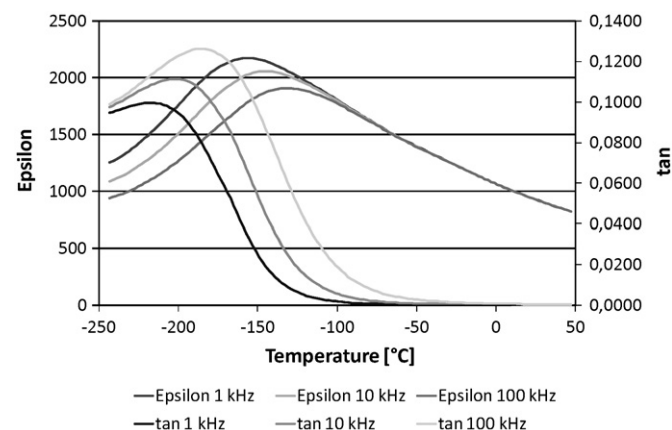

Fig. 11. Temperature dependence of the relative permittivity of $0.10(Bi_{0.5}Na_{0.5})TiO_3$–$0.90SrTiO_3$.

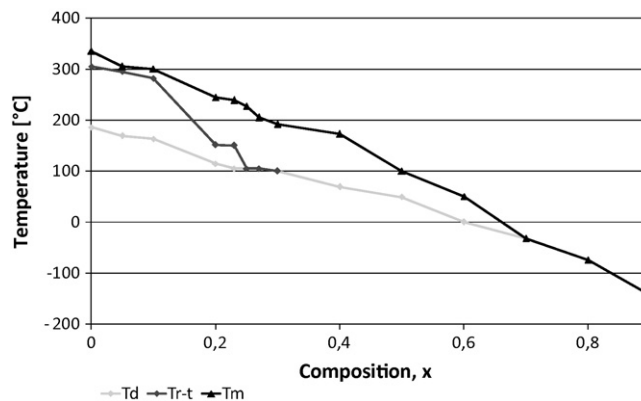Fig. 12. Dielectric transitions for $(1 - x)(Bi_{0.5}Na_{0.5})TiO_3$–$xSrTiO_3$.

$x = 0.6$ and $x = 0.7$ the depolarization temperature T_d decreases to $0\,^\circ C$. Up to $x = 0.7$ there is a non-polar phase between T_m and T_d. For higher strontium titanate content this non-polar phase disappears. In comparison to Watanabes phase diagram we observe T_d and $T_{r–t}$ in the range of $0.2 < x < 0.3$ to be approximately $70\,^\circ C$ higher.

Polarization and displacement curves (Fig. 13) illustrate the varying ferroelectric behavior at room temperature. Starting from ferroelectric behavior up to $x = 0.1$ (Fig. 13a and d) the systems shifts more and more towards antiferroelectric behavior (Fig. 13b and e). This supports the assumption that the non-polar phase between T_d and T_m is in fact antiferroelectric. Samples with $x > 0.4$ become paraelectric (Fig. 13c and f). This indicates that under high electric field (up to 6 kV/mm) the transition temperature T_d is shifted to lower temperatures.

In Fig. 14 the remnant polarization and the maximum polarization is drawn over the whole composition range. It illustrates a strong decrease in the remnant polarization at about $x = 0.25$. For $x > 0.5$ the remnant polarization approaches zero.

If the strain at room temperature is plotted against composition a pronounced strain maximum of 0.29% at $x = 0.25$ is found (Fig. 15), where Watanabe et al.[4] suggested the existence of a morphotropic phase boundary. For a similar system – $(1–x–y)(Bi_{0.5}Na_{0.5})TiO_3$–$xBaTiO_3$$y(Na_{0.5}K_{0.5})NbO_3$ – Zhang et al. suggest, that such a large strain is due to a combination of the lattice volume change caused by a field-induced AFE-FE phase transition and ferroelectric domain reorientation.[16] In another publication Zhang et al.[17] suggest that the reason for the large strain could be due to electrostriction.

To discuss this question we plotted the temperature dependence of the strain under maximum electric field for the composition $x = 0.2$ (Fig. 16). We observed two maxima, marked with arrows, which could be attributed to phase transitions at T_d and $T_{r–t}$. The first maximum would indicate a contribution of a ferroelectric/antiferroelectric phase transition. The second maximum would indicate a contribution from a structural transition (rhombohedral–tetragonal), which would be of certain relevance for the existence of a morphotropic phase boundary.

One can see from Fig. 16, that under high electric field there is a shift of both the depolarization temperature and the rhombohedral–tetragonal transition temperature of about $70\,^\circ C$ to lower temperatures in comparison to the
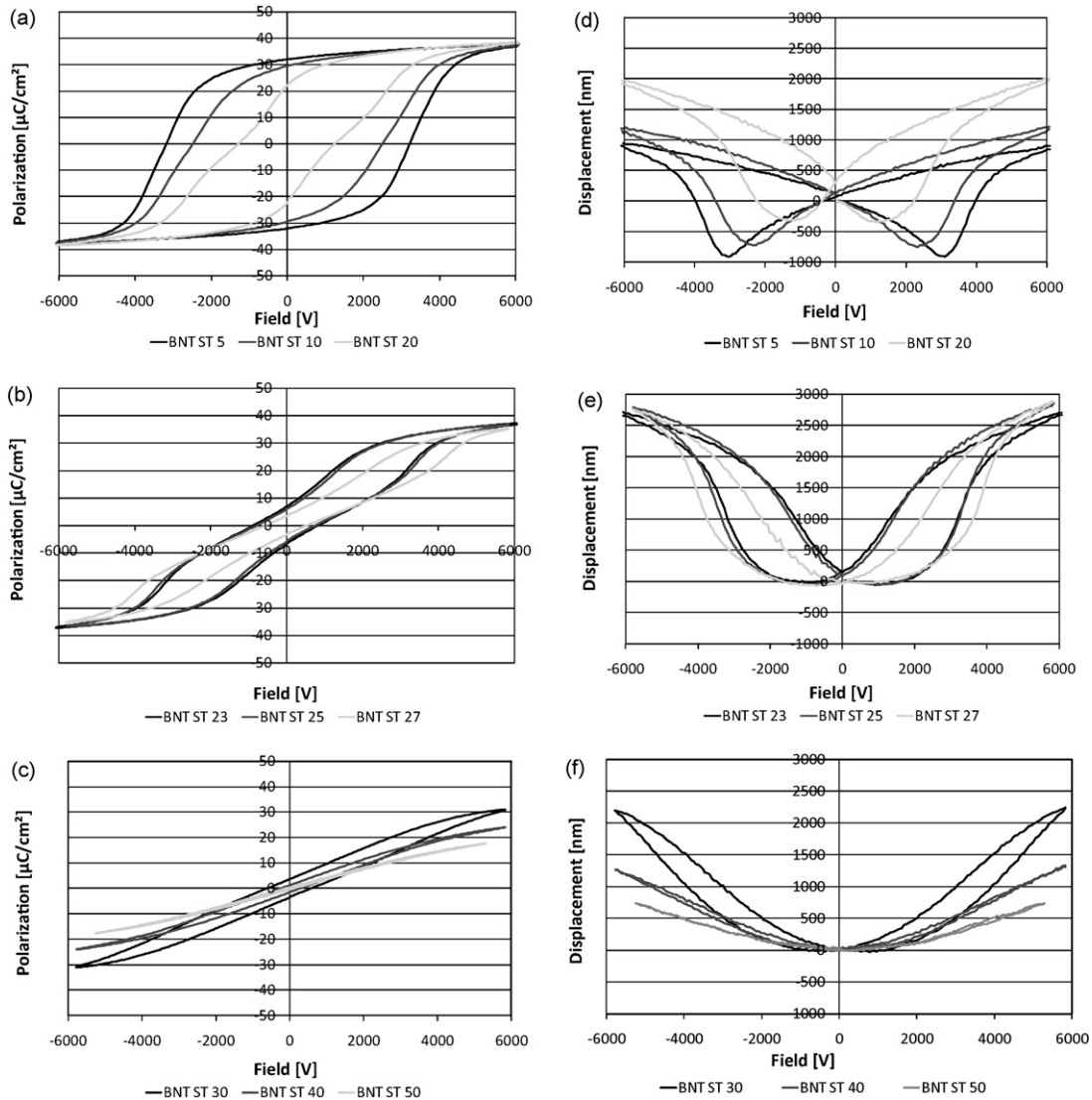
Fig. 13. Polarization and displacement curves for the system $(1 - x)(Bi_{0.5}Na_{0.5})TiO_3–xSrTiO_3$.

phase diagram drawn from the dielectric transitions for $(1 - x)(Bi_{0.5}Na_{0.5})TiO_3–xSrTiO_3$ (Fig. 12). This characteristics was observed also by Zhang et al.[16] in the system $(1–x–y)(Bi_{0.5}Na_{0.5})TiO_3–xBaTiO_3 y(Na_{0.5}K_{0.5})NbO_3$. This gives strong evidence that both phase transitions are field induced. The reason for the rhombohedral distortion of bismuth sodium titanate is most probably the formation of a covalent binding between the free electron pair of bismuth to a triple of the oxygen-atoms of the surrounding oxygen-dodecahedron being the reason for the A-site relaxor characteristics we observed
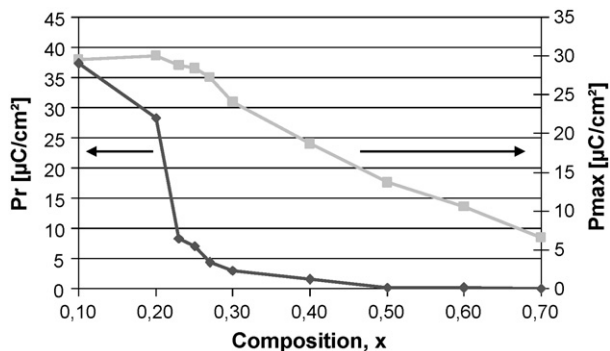

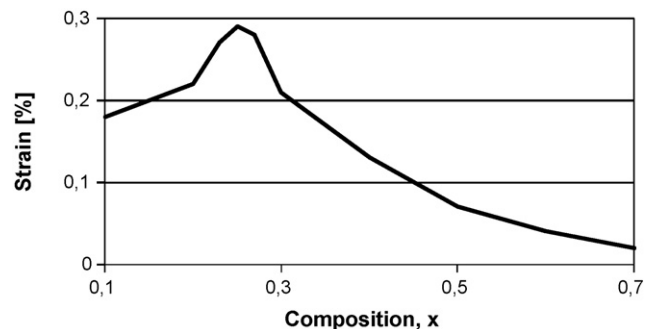Fig. 14. Remnant polarization (P_r) and maximum polarization (P_{max}) of the system $(1 - x)(Bi_{0.5}Na_{0.5})TiO_3–xSrTiO_3$.

Fig. 15. Maximum strain at room temperature for the system $(1 - x)(Bi_{0.5}Na_{0.5})TiO_3–xSrTiO_3$.
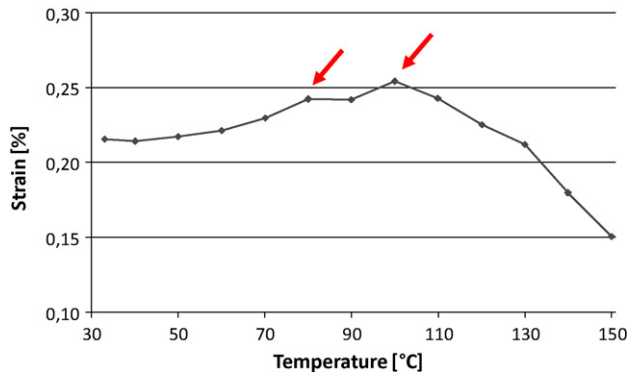
Fig. 16. Temperature dependence of the strain for $0.80(\text{Bi}_{0.5}\text{Na}_{0.5})\text{TiO}_3$–$0.20\text{SrTiO}_3$.

in this system (similar to lead containing relaxors, where an antiferroelectric ordering of the lead ions is observed[18]). Obviously the ordering induced by this covalent binding could be influenced either by an electrical field or temperature.

At the current status of our investigations we support the hypotheses stated by Zhang, since we did not find any structural features that hold up for a morphotropic phase boundary. In a very common sense the phase transition between ferroelectric and antiferroelectric phase at T_d or the supposed transition between a rhombohedral and a tetragonal phase at $T_{r–t}$ can be called a morphotropic phase boundary if only the maximum strain is considered a necessary attribute for it.

4. Conclusion

The phase diagram for $(1 − x)(\text{Bi}_{0.5}\text{Na}_{0.5})\text{TiO}_3$–$x\text{SrTiO}_3$ was completed between $x = 0$ and $x = 1$. No tetragonal distortion could be detected in the whole composition range. The lattice parameter (for cubic indexing) has a broad maximum at $x = 0.5$ contrary to the trend of ionic radii. Relaxor behavior was observed in all solid solutions (A-site relaxor). An antiferroelectric phase exists from pure $\text{Bi}_{0.5}\text{Na}_{0.5}\text{TiO}_3$ to a concentration of approximately $x = 0.7$. We support the hypothesis that the reason for the maximum strain of 0.29% at $x = 0.25$, which coincides with the transition from ferroelectric to antiferroelectric behavior, is a field-induced AFE-FE phase transition. A certain contribution of a structural transition (possibly rhombohedral–tetragonal) holds up for the existence of a morphotropic phase boundary.

Acknowledgements

References

1. Smolenskii GA, Isupov VA, Agranivyskaya AI, Krainik NN. New ferroelectrics of complex composition. IV. *Soviet Physics: Solid State* 1961;**2**:2651–4.
2. Rödel J, Jo W, Seifert K, Anton E, Granzow T, Damjanovic D. Perspective on the development of lead-free piezoceramics. *Journal of the American Ceramic Society* 2009;**92**:1153–77.
3. Hiruma Y, Watanabe Y, Nagata H, Takenaka T. Phase transition temperatures of divalent and trivalent ions substituted $(\text{Bi}_{1/2}\text{Na}_{1/2})\text{TiO}_3$ ceramics. *Key Engineering Materials* 2007;**350**:93–6.
4. Watanabe Y, Hiruma Y, Nagata H, Takenaka T. Phase transition temperature and electrical properties of divalent ions (Ca^{2+}, Sr^{2+} and Ba^{2+}) substituted $(\text{Bi}_{1/2}\text{Na}_{1/2})\text{TiO}_3$ ceramics. *Ceramics International* 2008;**34**: 761–4.
5. Takenaka T, Maruyama K, Sakata K. $(\text{Bi}_{1/2}\text{Na}_{1/2})\text{TiO}_3$–$\text{BaTiO}_3$ system for lead-free piezoelectric ceramics. *Japanese Journal of Applied Physics* 1991;**30**:2236–9.
6. Zuo R, Ye C, Fang X, Li J. Tantalum doped $0.94\text{Bi}_{0.5}\text{Na}_{0.5}\text{TiO}_3$–$0.06\text{BaTiO}_3$ piezoelectric ceramics. *Journal of the European Ceramic Society* 2008;**28**:871–7.
7. Lin D, Xiao D, Zhu J, Yu P. Piezoelectric and ferroelectric properties of lead-free $[\text{Bi}_{1−y}(\text{Na}_{1−x−y}\text{Li}_x)]0.5\text{Ba}_y\text{TiO}_3$ ceramics. *Journal of the European Ceramic Society* 2006;**26**:3247–51.
8. Yang Z, Liu B, Wei L, Hou Y. Structure and electrical properties of $(1 − x)\text{Bi}_{0.5}\text{Na}_{0.5}\text{TiO}_3$–$x\text{Bi}_{0.5}\text{K}_{0.5}\text{TiO}_3$ ceramics near morphotropic phase boundary. *Materials Research Bulletin* 2008;**43**:81–9.
9. Xu C, Lin D, Kwok KW. Structure, electrical properties and depolarization temperature of $(\text{Bi}_{0.5}\text{Na}_{0.5})\text{TiO}_3$–$\text{BaTiO}_3$ lead-free piezoelectric ceramics. *Solid State Sciences* 2008;**10**:934–40.
10. Sasaki A, Chiba T, Mamiya Y, Otsuki E. Dielectric and piezoelectric properties of $(\text{Bi}_{0.5}\text{Na}_{0.5})\text{TiO}_3$–$(\text{Bi}_{0.5}\text{K}_{0.5})\text{TiO}_3$ systems. *Japanese Journal of Applied Physics* 1999;**38**:5564–7.
11. Shieh J, Wu KC, Chen CS. Switching characteristic of MPB compositions of $(\text{Bi}_{0.5}\text{Na}_{0.5})\text{TiO}_3$–$\text{BaTiO}_3$–$(\text{Bi}_{0.5}\text{K}_{0.5})\text{TiO}_3$ lead-free ferroelectric ceramics. *Acta Materialia* 2007;**55**:3081–7.
12. Jauch W, Palmer A. Anomalous zero-point motion in SrTiO_3: results from γ-ray diffraction. *Physical Review B* 1999:2961–3.
13. Hiruma Y, Nagata H, Takenaka T. Thermal depoling process and piezoelectric properties of bismuth sodium titanate ceramics. *Journal of Applied Physics* 2009;**105**.
14. Hiruma Y, Imai Y, Watanabe Y, Nagata H, Takenaka T. Large electrostrain near the phase transition temperature of $(\text{Bi}_{0.5}\text{Na}_{0.5})\text{TiO}_3$–$\text{SrTiO}_3$ ferroelectric ceramics. *Applied Physics Letters* 2008;**92**.
15. Park S-E, Hong KS. Variations of structure and dielectric properties on substituting A-site cations for Sr^{2+} in $(\text{Na}_{1/2}\text{Bi}_{1/2})\text{TiO}_3$. *Journal of Materials Research* 1997;**12**:2152–7.
16. Zhang S, Kounga AB, Aulbach E, Granzow T, Jo W, Kleebe HJ, et al. Lead-free piezoceramics with giant strain in the system $\text{Bi}_{0.5}\text{Na}_{0.5}\text{TiO}_3$–$\text{BaTiO}_3$–$\text{K}_{0.5}\text{Na}_{0.5}\text{NbO}_3$. I. Structure and room temperature properties. *Journal of Applied Physics* 2008;**103**.
17. Zhang S, Kounga AB, Jo W, Jamin C, Seifert K, Granzow T, et al. High-strain lead-free antiferroelectric electrostrictors. *Advanced Materials* 2009;**21**:1–5.
18. Chen IW, Li P, Wang Y. Structural origin of relaxor perovskites. *Journal of Physics and Chemistry of Solids* 1995;**57**:1525–36.